

Ultra-fast underwater suction traps

Olivier Vincent¹, Carmen Weißkopf², Simon Poppinga²,
Tom Masselter², Thomas Speck², Marc Joyeux¹,
Catherine Quilliet¹ and Philippe Marmottant^{1,*}

¹Laboratoire Interdisciplinaire de Physique, UMR 5588 CNRS and University of Grenoble 1, 140 Avenue de la Physique, 34802 Saint Martin d'Hères Cedex, France

²Plant Biomechanics Group Freiburg, Botanic Garden, Faculty of Biology, University of Freiburg, Schänzlestrasse 1, 79104 Freiburg im Breisgau, Germany

Carnivorous aquatic *Utricularia* species catch small prey animals using millimetre-sized underwater suction traps, which have fascinated scientists since Darwin's early work on carnivorous plants. Suction takes place after mechanical triggering and is owing to a release of stored elastic energy in the trap body accompanied by a very fast opening and closing of a trapdoor, which otherwise closes the trap entrance watertight. The exceptional trapping speed—far above human visual perception—impeded profound investigations until now. Using high-speed video imaging and special microscopy techniques, we obtained fully time-resolved recordings of the door movement. We found that this unique trapping mechanism conducts suction in less than a millisecond and therefore ranks among the fastest plant movements known. Fluid acceleration reaches very high values, leaving little chance for prey animals to escape. We discovered that the door deformation is morphologically predetermined, and actually performs a buckling/unbuckling process, including a complete trapdoor curvature inversion. This process, which we predict using dynamical simulations and simple theoretical models, is highly reproducible: the traps are autonomously repetitive as they fire spontaneously after 5–20 h and reset actively to their ready-to-catch condition.

Keywords: bladderwort; carnivorous/insectivorous plants; suction mechanism
functional morphology; fluid dynamics; *Utricularia*

1. INTRODUCTION

Bladderworts (*Utricularia* spp., Lentibulariaceae) are carnivorous as an adaptation to nutrient-poor habitats [1–4]. The genus comprises more than 220 species with an almost worldwide distribution and exhibits different life forms [4,5]. As probably the most extreme embodiment of the carnivorous syndrome [3], all species are completely rootless, and at least all aquatic species feature a suction trap mechanism that relies on a release of stored elastic energy in the trap body. Entailing a cascade of fast motions [6–15], the whole trapping action is too fast to be followed with the naked eye. Yet there are no detailed camera recordings available, and the exact motion pattern has been unclear until now. In order to understand how the trapdoor opens, and to elucidate the dynamics of the motion sequences involved, we studied traps of three aquatic species: *Utricularia australis* R.Br., *U. inflata* Walter and *U. vulgaris* L. All species belong to the infrageneric section *Utricularia* [5,16], which shows, as far as known, a homogeneous trap architecture [17] with (as to its functional morphology) a nearly identical trapping mechanism. Trap diameters range from 0.5 to 3 mm [5,17].

The lenticular *Utricularia* trap (figure 1a and electronic supplementary material, S1) works with a two-phase mechanism [2,3]. During the first slow phase, which lasts about 1 h, internal glands actively pump water out

of the trap interior, so that elastic energy is stored in the trap body owing to a lower internal hydrostatic pressure. In this set condition, when ready for catch, the trap shows concave wall curvatures (figure 1b). A flexible door with protruding trigger hairs closes the entrance watertight. Prey animals can stimulate these hairs and thereby launch the second, ultra-fast phase, which runs passively because of a mechanical conversion of elastic energy into kinetic energy. The triggering results in door opening, trap wall relaxation and water (and thereby prey) influx due to the sudden increase of the trap volume (figure 1c). After the door is closed, the prey is dissolved by digestive enzymes secreted by quadrifid glands, and nutrients are absorbed by the plant. Both phases together form a repeatable 'active slow deflation–passive fast suction' sequence (figure 1b and electronic supplementary material, movies S1 and S2).

2. MATERIAL AND METHODS

(a) Experiments

We investigated traps (2–3 mm in diameter) of the species *U. inflata*, *U. vulgaris* and *U. australis*. The motion was studied with a high-performance light microscope (Olympus IX70) and stereo microscopes (Zeiss DV8, Olympus SZX9; up to 85.5× magnification). Trapping actions were recorded with up to 15 000 frames s⁻¹ (high-speed cameras Vision Research Phantom Miro 4 and Olympus i-Speed 3). Particles used to track the flow were hollow glass spheres with a diameter in the range of 2–20 μm and a density of 1.1 g cm⁻³

*Author for correspondence (philippe.marmottant@ujf-grenoble.fr).

Electronic supplementary material is available at <http://dx.doi.org/10.1098/rspb.2010.2292> or via <http://rspb.royalsocietypublishing.org>.

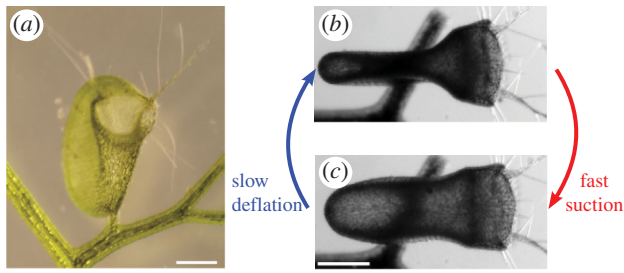


Figure 1. Traps of *U. inflata*. (a) Frontal view of a trap; the concave walls and the entrance are clearly visible. (b,c) Top views of a trap (the door facing to the right) showing the two-phase trap mechanism (b) before and (c) after firing. The scale bar is 500 μm .

(Polysciences, Inc.). Laser sheet fluorescence microscopy [18] was used to observe the median trapdoor axis (laser sheet approx. 10 μm thick) of a trap directly, previously infused in rhodamine dye for a few minutes. Scanning electron microscopy (SEM) imaging involved the following preparation steps: dehydration of specimen with methanol substitution, critical-point drying with a Bal-Tec CPC 030 and gold coating (approx. 15 nm) with a Cressington Sputter Coater 108 auto. The SEM LEO 435 VP was used.

(b) Time measurements

The different steps during trapdoor opening in *U. inflata* and *U. vulgaris* were found to vary in duration. We recorded 16 openings with at least 3000 fps. (i) Buckling (see §3) duration varied between 0.7 and 21 ms (2 ms on average). We interpret this wide range to be the consequence of variations in pressure values before triggering or different frictions on the threshold. (ii) Opening lasts between 0.4 and 0.8 ms (0.5 ms on average). (iii) The closure took between 1 and 5.5 ms (2.5 ms on average) with a small proportion of curvature remaining. Final resetting of the trapdoor took between 0.5 and 300 ms.

(c) Elastic shell simulations

The trap body and trapdoor are modelled as elastic shells of thickness h , Young's modulus of elasticity E and Poisson ratio ν . Their potential energy U_{pot} is the sum of a bending term, U_{bend} , and a stretching term, U_{stretch} [19], such that

$$U_{\text{bend}} = \frac{Eh^3}{24(1-\nu^2)} \int_S [(\text{Tr}(\mathbf{b}))^2 - 2(1-\nu)\text{Det}(\mathbf{b})] dS \quad (2.1)$$

and

$$U_{\text{stretch}} = \frac{Eh}{2(1-\nu^2)} \int_S [\nu(\text{Tr}(\boldsymbol{\epsilon}))^2 + (1-\nu)\text{Tr}(\boldsymbol{\epsilon}^2)] dS, \quad (2.2)$$

with \mathbf{b} as the difference between the strained and unstrained local curvature tensors, and $\boldsymbol{\epsilon}$ as the two-dimensional Cauchy-Green local strain tensor. The integrals are evaluated on the surface S of the shell. It is assumed that the material is incompressible, which implies that $\nu = 0.5$. All surfaces are described as triangular meshes (figure 2a).

The body of the *Utricularia* trap is modelled as a closed shell with a realistic shape (larger radius 1 mm, thickness $h = h_{\text{body}} = 60 \mu\text{m}$). The initial shape holds a portion of surface with negative curvature (figure 1), ensuring a smooth deflation. Simulations are performed by decreasing the inner volume V quasi-statically, and by searching for each volume the geometry that minimizes the potential energy U_{pot} using SURFACE EVOLVER freeware [20]. The pressure

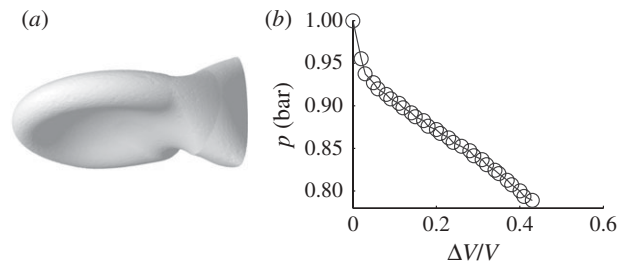


Figure 2. Simulated trap body and pressure values. (a) Simulation of the *U. inflata* trap body (the entrance facing rightwards) as an elastic shell, assuming the initial shape of the swollen trap. Owing to water removal, its sides become concave. The door is not modelled. (b) Pressure inside the *U. inflata* trap as a function of deflation, as computed in simulations. The Young modulus of the shell is $E = 20 \text{ MPa}$, the shell thickness is $h = 60 \mu\text{m}$ and the largest radius is 1 mm.

difference Δp between the inside and the outside of a trap is expressed by $\Delta p = -d(\min(U_{\text{pot}}))/dV$. The Young modulus, $E = E_{\text{body}}$, is determined by requiring the inner volume V to be reduced by about 40 per cent for $\Delta p = 15 \text{ kPa}$ [12,14].

The *Utricularia* trapdoor is modelled as a quarter of a prolate ellipsoid, with a polar radius of 300 μm and an equatorial radius of 240 μm , the pole axis joining the sides of the trap, and a thickness $h_{\text{door}} = 30 \mu\text{m}$ (figure 4d-f). One of the borders of the ellipsoid represents the trapdoor frame and is kept fixed, whereas the lower edge is free to move. During the dynamic simulation, the pressure inside the trap is slowly decreased from atmospheric pressure, and the position \mathbf{r}_k of each vertex k of the mesh is updated according to a Langevin equation:

$$m_k \frac{d^2 \mathbf{r}_k}{dt^2} = -\nabla U_{\text{pot}} - \Delta p \delta A_k \mathbf{n}_k - m_k \gamma \frac{d\mathbf{r}_k}{dt} + \sqrt{2m_k \gamma k_B T} \frac{dW(t)}{dt}, \quad (2.3)$$

with m_k as the mass of the vertex, δA_k as the element of surface that surrounds vertex k , \mathbf{n}_k the outward normal to the surface, k_B the Boltzmann constant, T the ambient temperature and $W(t)$ a Wiener process. The first and second terms in the right-hand side of this equation describe elastic and pressure forces, respectively, while the last two terms model the effects of the liquid, namely friction and thermal noise, even if the full motion of the fluid around the trap is not modelled. The dissipation coefficient γ is assumed to be $2 \times 10^5 \text{ s}^{-1}$. Thermal noise happens to be orders of magnitude smaller than elastic forces, and was introduced for the sake of completeness. A constant pressure difference is imposed in order to model the first phase of opening (after full opening, the pressure difference relaxes). When assuming $E_{\text{door}} = 2.7 \text{ MPa}$, one observes that the shape of the door remains essentially unchanged up to $\Delta p = 15.5 \text{ kPa}$.

Complete details of these simulations are provided in a separate paper [21].

(d) Prediction of pressure for door buckling

Using scaling arguments, the buckling pressure of a spherical shell [22] is approximately given by:

$$P_{\text{buckling}} \sim E_{\text{door}} \left(\frac{h_{\text{door}}}{R_{\text{door}}} \right)^2, \quad (2.4)$$

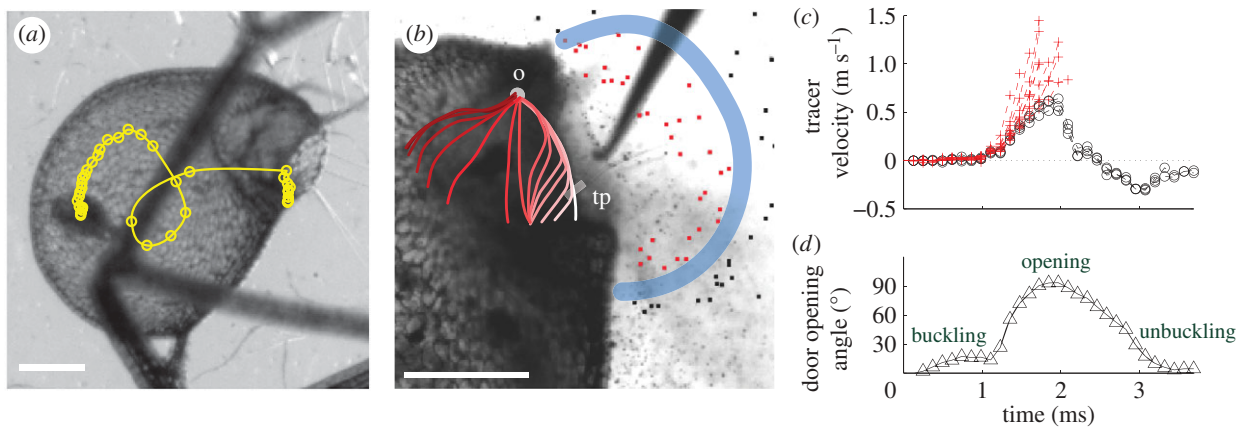


Figure 3. Suction dynamics in *U. inflata*. (a) Fast suction of a small crustacean (*Cyclops* sp.): the circles denote the position of its centre at time intervals of 0.34 ms. (b) Detail of the valve profile before suction (side view), with tracer particles suspended in the fluid. The thick blue line delimitates the aspiration zone: only particles within the zone (tagged in red) are 'trapped'. Manual triggering is performed with a needle. We also superimposed a sketch of the median door axis progression during firing, as observed in video images (see also figure 4). The progression is displayed using different red scale values, with the lightest white value indicating the initial profile. Each step depicts a 0.34 ms time lag. tp, trigger hair insertion point; o, pivot point (see also (d)). (c) Influx velocity of tracer particles. Red crosses indicate 'trapped' particles, black crosses indicate 'untrapped' particles. Lines are interrupted at trap entrance. (d) Temporal angular change of the trigger hair insertion point (tp) during door firing, with the pivot point (o), in relation to its original position when the trap is set. The scale bar is 500 μm .

with R_{door} the typical radius of curvature of the door and h_{door} the thickness of the door.

(e) Prediction of the duration of trap inflation

The trap is mechanically equivalent to a mass-spring system, initially under compression, that is suddenly released. The spring to consider arises from the elasticity of the trap body, and its stiffness k resulting from the force squeezing the sides $k\Delta e = S\Delta p$, with $\Delta e = 0.5$ mm the change in width and $S = 1$ mm² the area of each side. The mass m_a is that of the displaced fluid, which is comparable to the total mass of fluid in the trap after firing (volume in the order of 1 mm³). This mass-spring system relaxes with a characteristic inertial time $\tau = 2\pi(m_a/k)^{1/2} = 1$ ms, comparable to the recorded time of suction (1 ms).

3. RESULTS AND DISCUSSION

Although the first phase (active slow deflation; figure 1b) has already been documented in terms of deflated volume and internal pressure [12], the elastic shell simulations presented here allow us to estimate the stiffness of the trap body. The trap body is characterized by a Young's modulus in the range of 5–20 MPa (figure 2; electronic supplementary material, movie S3), which is in the range of that of fully turgescient parenchymatous tissues [23]. It is two cell layers thick, mostly flexible and therefore accounts for the deformation in the deflation phase.

The second phase comprises trap wall relaxation and trapdoor opening/closure (figure 1c). We investigated suction dynamics and trapdoor movement, using high-speed video imaging with up to 15 000 frames s⁻¹, and digital particle tracking. Several capture events of small crustaceans (freshwater copepods of the genus *Cyclops*) were recorded. Caught animals looping within the traps indicated that swirls develop inside (figure 3a; electronic supplementary material, movie S4). We hypothesize that these swirls, despite not being investigated here, are crucial for prey retention and caused by the inner trap

structure. The trapping sequence lasts for only a few milliseconds. The time span of suction itself is half a millisecond, which is much shorter than previously estimated [3,12]. *Utricularia* therefore features the fastest trapping movement of all carnivorous plants, ranking even among the fastest movements generally known in the plant kingdom [24–28]. The suction time after trapdoor opening can be estimated with simple arguments based on the trap body elasticity and the mass of water displaced (see §2). The fluid speed was deduced by tracking small glass beads (figure 3b,c). We recorded a maximum fluid velocity of 1.5 m s⁻¹, implying that liquid inertia forces are well above viscous forces (the ratio of these forces—the Reynolds number—reaches 900), and measured a maximum fluid acceleration of 600g.

The swiftness of the suction is enabled by the extremely fast opening and closure of the door, which acts as a flexible valve [2,9,10]. Our high-speed video recordings in fluorescence laser sheet microscopy reveal the following sequence (figure 3b,d; electronic supplementary material, movies S5–S7) after manually triggering the trap with a fine needle. (i) *Inversion of the door curvature*: the convex trapdoor—in the 'ready to catch' condition—bulges inside, starting at the region of trigger hair insertion. This inversion of curvature then spreads progressively over the door surface (figure 4a,b), with the door still being closed. In this phase, the trigger hairs converge and flap against the door, so they do not block the trap entrance during step two. (ii) *Opening*: the door swings inside rapidly (figure 4c), in approximately 0.5 ms on average. (iii) *Door resetting*: the door quickly moves back in about 2.5 ms on average. A large proportion of inverted curvature remains, then disappears as the door gets back to its initial position. The duration for a total curvature resetting may be as fast as 0.5 ms, or as slow as 300 ms in some cases.

The fast opening and closing of the door, with an abrupt change in shape, strongly suggests that the underlying principle is a buckling [24] of an elastic valve. We

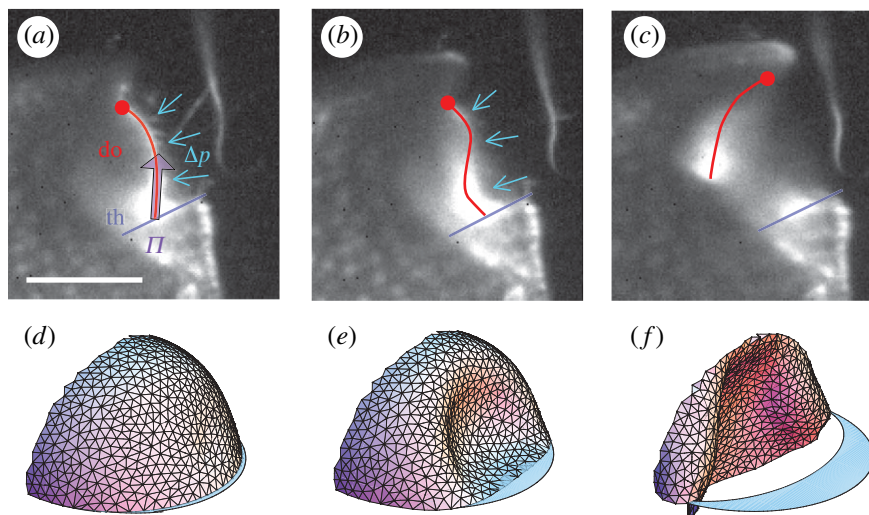


Figure 4. Inversion of trapdoor curvature in *U. inflata*. (a–c) Buckling of the median door axis, visualized by light sheet fluorescence microscopy. (a) Initially the trapdoor is convex towards the outside of the trap. The force exerted on the door surface owing to water pressure difference Δp between the interior of the trap and the outer medium is balanced by the friction force Π , exerted by the threshold (th) on the trapdoor (do). (b) Following excitation, the trapdoor becomes gradually concave on its outer side, starting at the trigger hair insertion point. The free edge of the trapdoor is pulled away from the threshold contact area by water pressure. (c) Consequently, the door opens wide. (d)–(f) Dynamic simulation of the trapdoor. Parts (d) and (e) correspond to (a) and (b), respectively, while (f) shows the door only half-way from complete inversion. The scale bar is 500 μm .

hypothesize that after the trap is set the internal/external pressure difference is close to the critical pressure for spontaneous buckling, and a slight disturbance suffices to trigger the motion. The triggering could be entirely mechanical (trigger hairs acting as levers) [2,9], but we cannot exclude an excitatory step (physiological sensitivity) that would help to exceed the remaining mechanical activation barrier [12]. The door buckles prior to opening, contrary to the previous assumption that opening starts before buckling [2,9]. After trap inflation, the inside and outside pressures are levelled, and the door unbuckles to its initial state of curvature, thereby closing the trap. Note that such large door displacements involve relatively small surface strains of the door: it can be estimated that the longitudinal strain of the outer surface is $h_{\text{door}}/R_{\text{door}} \approx -0.1$ when achieving full curvature inversion, and the opposite for the inner surface.

This buckling hypothesis is well supported by our dynamic simulations. We modelled the *Utricularia* door as a quarter-ellipsoidal shell (see §2). One border of the ellipsoid is fixed, whereas the other border (free edge) is in frictionless contact with a threshold. The shell has both bending and stretching energy. We performed dynamics simulations while the pressure inside the trap was slowly decreased. We noticed that the door shape changes very little up to a pressure difference of 15.5 kPa. Buckling then spontaneously occurs, with the door sliding along the threshold and swinging open, in excellent concordance with our high-speed videos of the actual trapdoor (figure 4d–f; electronic supplementary material, movie S8). When the pressure difference is just lower than this critical value, the trap is stable, but the energy barrier to trigger buckling is low, making the trap extremely sensitive to external perturbation.

Independently from simulations, the buckling mechanism entails a general estimation for door and body wall thicknesses in *Utricularia*. The door should be thin enough so that it buckles owing to underpressure

generated by active pumping of water out of the trap. Furthermore, we can hypothesize that in order to suck a maximum amount of water and thereby prey, mechanical and geometrical parameters of the body walls and the door should be optimized so that the body reaches a nearly whole deflation when submitted to the underpressure. Too stiff a body would not deform enough, and hence would suck too small an amount of water, while too soft a body would hardly overcome viscous dissipation, and would then not be fast enough during entrapping suction. The elastic energy at a maximum deflation, in the order of $E_{\text{body}} h_{\text{body}}^3$ (according to equation (2.1), using a deformation of relative amplitude 1), should therefore be equal to the work generated by pressure at buckling, in the order of $P_{\text{buckling}} R^3$, with R being the typical size of the trap. Using the scaling expression for the buckling pressure (equation (2.4)), we predict the following door-to-body thickness ratio:

$$\frac{h_{\text{door}}}{h_{\text{body}}} \sim \left(\frac{h_{\text{body}}}{R} \right)^{1/2} \left(\frac{E_{\text{body}}}{E_{\text{door}}} \right)^{1/2}. \quad (3.1)$$

Such a ratio is smaller than 1, because the thickness h_{body} is much smaller than the size of the trap R , and because the range of Young's moduli for parenchymatous tissues does not extend over several orders of magnitude. We therefore conclude that doors of aquatic *Utricularia* are thinner than their body, with a door thickness optimized to open at a maximum deflation. This result should be important for the consideration of trap functioning in other *Utricularia* species where the suction mechanism is doubtful, such as in the terrestrial *U. multifida* [17].

Furthermore, we found that aquatic *Utricularia* traps can fire spontaneously, corroborating a hypothesis reported in Peroutka *et al.* [29] by continuously imaging a single trap during 20 days. We observed more than 60 successive spontaneous suction during this time span,

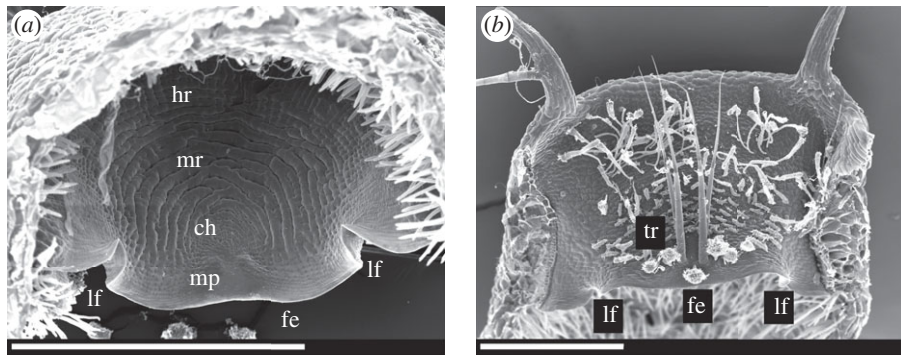


Figure 5. Standard electron microscopy micrographs of dissected *U. vulgaris* trapdoors. The lateral folds are clearly visible. ch, central hinge; fe, free edge; lf, lateral fold; hr, hinge region; mp, middle piece; mr, middle region; tr, trigger hairs. (a) Interior view. (b) Exterior view. The scale bar in both figures is 500 μm .

assuming that tiny swimming organisms like algae are not capable of triggering the mechanism [30]. Traps activate on average at time intervals between 5 and 20 h (electronic supplementary material, figure S2 and movie S2). This observation (also reported by Adamec [31]) confirms the buckling scenario: the pressure inside the trap reaches a low value that entails buckling, probably owing to mechanical/thermal noise.

Looking in detail at the trapdoor morphology, we found how it is optimized for fast buckling and unbuckling. The roughly semicircular door is fixed to the upper part of the trap entrance along a curved arch. It rests with its free edge on the lower part of the entrance (i.e. the threshold; electronic supplementary material, figure S1). Here, mucilage is secreted and, in combination with an exfoliated cuticle (velum), a watertight seal is achieved [2,3]. We noticed that the free edge of the door always features two conspicuous lateral folds (figure 5), which presumably add displacement space by unfolding.

The trapdoor consists of two differing cell layers. Those of the inner layer are elongated and radially arranged around the central hinge region (figure 5a). The most noticeable feature is the pattern of concentric circular lines, indicating constrictions of the cells in this middle region. These cells have been assumed to function like compressive bellows [2,3]. In addition, considering the observed deformation, we suggest that these constrictions act as pre-folds, increasing flexibility in the radial direction. This would channel the reversible buckling/unbuckling process and enforce it to follow the same reproducible deformation pattern. Buckling starts in the thickened middle piece below the thin central hinge region, resulting in trigger hair converging and flapping against the door. The hinge region along the curved arch is characterized by radially arranged cells without constrictions. This region is less affected by deformation and might serve as a spring-like structure for closing the door. In contrast, the outer cell layer of the door is not distinctly compartmentalized and features smaller cells, running parallel to each other (figure 5b).

In conclusion, our investigations show how buckling and unbuckling lead to door opening and closure, which is associated with a suction swirl. This differs from the mechanism of the Venus flytrap (*Dionaea muscipula*), described as ‘snap buckling’ [27], where a one-way internal buckling results in the trapping movement. The remarkable valve mechanism of *Utricularia*

should provide inspiration for a great variety of biomimetic applications, especially for new deployable materials and fluid-elastic structures designed to act repeatedly, such as in microfluidic devices. On a biological level, the repetitive spontaneous valve buckling and opening could account for reports on phytoplankton, bacterial communities and detritus regularly found in traps [29,30,32,33]. Usually considered as ‘bycatch’, there is evidence that they play an important role in *Utricularia* nutrient supply [32–36]. The evolutionary success of these carnivorous plants might be explained by the fact that their traps are not only active, but also autonomous: this character could facilitate the rootless *Utricularia* plants to colonize nutrient-poor habitats.

P.M. wishes to thank Clément Nizak for his help in setting up the Laser sheet fluorescence microscopy. S.P. would like to thank Lubomir Adamec, Trebon (Czech Republic) for providing plant material.

REFERENCES

- 1 Darwin, C. 1875 *Insectivorous plants*. London, UK: Murray.
- 2 Lloyd, F. E. 1942 *The carnivorous plants*. Waltham, MA: Chronica Botanica.
- 3 Juniper, B. E., Robins, R. J. & Joel, D. M. 1989 *The carnivorous plants*. London, UK: Academic.
- 4 Barthlott, W., Porembski, S., Seine, R. & Theisen, I. 2008 *The curious world of carnivorous plants: a comprehensive guide to their biology and cultivation*. Portland, OR: Timber.
- 5 Taylor, P. 1989 *The genus Utricularia: a taxonomic monograph*. London, UK: Royal Botanic Gardens, Kew.
- 6 Treat, M. 1875 Is the valve of *Utricularia* sensitive? *Harper's New Monthly Magazine* **52**, 382–387.
- 7 Czaja, A. T. 1922 Die Fangvorrichtung der *Utricularia*-blase. *Z. Bot.* **14**, 705–729.
- 8 Ekambaram, T. 1924 Note on the mechanism of the bladders of *Utricularia*. *J. Ind. Bot. Soc.* **4**, 73–74.
- 9 Lloyd, F. E. 1932 Is the door of *Utricularia* an irritable mechanism? *Can. J. Bot.* **10**, 780–786.
- 10 Lloyd, F. E. 1929 The mechanism of the water tight door of the *Utricularia* trap. *Plant Physiol.* **4**, 87–102. (doi:10.1104/pp.4.1.87)
- 11 Diannelidis, T. & Umrath, K. 1953 Aktionsströme der Blase von *Utricularia vulgaris*. *Protoplasma* **42**, 58–62. (doi:10.1007/BF01248655)
- 12 Sydenham, P. & Findlay, G. 1973 The rapid movement of the bladder of *Utricularia* sp. *Aust. J. Biol. Sci.* **26**, 1115–1126.

- 13 Withycombe, C. L. 1924 On the function of the bladders of *Utricularia*. *J. Linn. Soc.* **46**, 401–413.
- 14 Sasago, A. & Sibaoka, T. 1985 Water extrusion in the trap bladders of *Utricularia vulgaris*. I. A possible pathway of water across the bladder wall. *Bot. Mag. Tokyo* **98**, 55–66. (doi:10.1007/BF02488906)
- 15 Sasago, A. & Sibaoka, T. 1985 Water extrusion in the trap bladders of *Utricularia vulgaris*. II. A possible mechanism of water outflow. *Bot. Mag. Tokyo* **98**, 113–124. (doi:10.1007/BF02488791)
- 16 Müller, K. & Borsch, T. 2005 Phylogenetics of *Utricularia* (Lentibulariaceae) and molecular evolution of the trnK intron in a lineage with high substitutional rates. *Plant Syst. Evol.* **250**, 39–67. (doi:10.1007/s00606-004-0224-1)
- 17 Reifenrath, K., Theisen, I., Schnitzler, J., Porembski, S. & Barthlott, W. 2006 Trap architecture in carnivorous *Utricularia* (Lentibulariaceae). *Flora* **201**, 597–605. (doi:10.1016/j.flora.2005.12.004)
- 18 Reynaud, E. G., Krzic, U., Greger, K. & Stelzer, E. H. K. 2008 Light sheet-based fluorescence microscopy: more dimensions, more photons, and less photodamage. *HFSP J.* **2**, 266–275. (doi:10.2976/1.2974980)
- 19 Komura, S., Tamura, K. & Kato, T. 2005 Buckling of spherical shells adhering onto a rigid substrate. *Eur. Phys. J.* **18**, 343–358. (doi:10.1140/epje/e2005-00038-5)
- 20 Brakke, K. 1992 The surface evolver. *Exp. Math* **1**, 141–165.
- 21 Joyeux, M., Vincent, O. & Marmottant, P. In press. Mechanical model of the ultra-fast underwater trap of *Utricularia*. *Phys. Rev. E*.
- 22 Landau, L. D. & Lifshitz, E. M. 1986 *Theory of elasticity*. Oxford, UK: Pergamon.
- 23 Niklas, K. J. 1988 Dependency of the tensile modulus on transverse dimensions, water potential, and cell number of pith parenchyma. *Am. J. Bot.* **75**, 1286–1292. (doi:10.2307/2444450)
- 24 Skotheim, J. M. & Mahadevan, L. 2005 Physical limits and design principles for plant and fungal movements. *Science* **308**, 1308–1310. (doi:10.1126/science.1107976)
- 25 Edwards, J., Whitaker, D., Klionsky, J. & Lasbowski, M. L. 2005 A record breaking pollen catapult. *Nature* **435**, 164. (doi:10.1038/435164a)
- 26 Nicholson, C. C., Bales, J. W., Palmer-Fortune, J. E. & Nicholson, R. G. 2008 Darwin's bee-trap: the kinetics of *Catasetum*, a New World orchid. *Plant Signal Behav.* **3**, 19–23. (doi:10.4161/psb.3.1.4980)
- 27 Forterre, Y., Skotheim, J. M., Dumais, J. & Mahadevan, L. 2005 How the Venus Flytrap snaps. *Nature* **433**, 421–425. (doi:10.1038/nature03185)
- 28 Taylor, P. E., Card, G., House, J., Dickinson, M. H. & Flagan, R. C. 2006 High-speed pollen release in the white mulberry tree, *Morus alba* L. *Sex Plant Reprod.* **19**, 19–24. (doi:10.1007/s00497-005-0018-9)
- 29 Peroutka, M., Adlassnig, W., Volgger, M., Lendl, T., Url, W. G. & Lichtscheidl, I. K. 2008 *Utricularia*: a vegetarian carnivorous plant? *Plant Ecol.* **199**, 153–162. (doi:10.1007/s11258-008-9420-3)
- 30 Alkhalaf, I., Hübener, T. & Porembski, S. 2009 Prey spectra of aquatic *Utricularia* species (Lentibulariaceae) in Northeastern Germany: the role of planktonic algae. *Flora* **204**, 700–708. (doi:10.1016/j.flora.2008.09.008)
- 31 Adamec, L. 2010 The comparison of mechanically stimulated and spontaneous firings in traps of aquatic carnivorous *Utricularia* species. *Aquat. Bot.* **94**, 44–49. (doi:10.1016/j.aquabot.2010.09.004)
- 32 Gordon, E. & Pacheco, S. 2007 Prey composition in the carnivorous plants *Utricularia inflata* and *U. gibba* (Lentibulariaceae) from Paria Peninsula, Venezuela. *Rev. Biol. Trop. (Int. J. Trop. Biol.)* **55**, 795–803.
- 33 Albert, V. A., Jobson, R. W., Michael, T. P. & Taylor, D. J. 2010 The carnivorous bladderwort (*Utricularia*, Lentibulariaceae): a system inflates. *J. Exp. Bot.* **61**, 5–9. (doi:10.1093/jxb/erp349)
- 34 Sirova, D., Adamec, L. & Vrba, J. 2003 Enzymatic activities in traps of four aquatic species of the carnivorous genus *Utricularia*. *New Phytol.* **159**, 669–675. (doi:10.1046/j.1469-8137.2003.00834.x)
- 35 Sirova, D., Borovec, J., Santruckova, H., Santrucek, J., Vrba, J. & Adamec, L. 2009 *Utricularia* carnivory revisited: plants supply photosynthetic carbon to traps. *J. Exp. Bot.* **61**, 99–103. (doi:10.1093/jxs/erb286)
- 36 Sirova, D., Borovec, J., Cerna, B., Rejmankova, E., Adamec, L. & Vrba, J. 2009 Microbial community development in the traps of aquatic *Utricularia* species. *Aquat. Bot.* **90**, 129–136. (doi:10.1016/j.aquabot.2008.07.007)